



A Monte Carlo Methodology for Environmental Assessment Applied to Offshore Processing of Natural Gas with High Carbon Dioxide Content

Cristiane S. B. Gonzaga^{*1}, Ofélia de Q. F. Araújo², José L. de Medeiros³

¹School of Chemistry, Federal University of Rio de Janeiro, CT, E, Ilha do Fundão, Rio de Janeiro, RJ, 21941-909, Brazil

e-mail: crissbg@gmail.com

²School of Chemistry, Federal University of Rio de Janeiro, CT, E, Ilha do Fundão, Rio de Janeiro, RJ, 21941-909, Brazil

e-mail: ofelia@eq.ufrj.br

³School of Chemistry, Federal University of Rio de Janeiro, CT, E, Ilha do Fundão, Rio de Janeiro, RJ, 21941-909, Brazil

e-mail: jlm@eq.ufrj.br

Cite as: Gonzaga, C. S. B., Araújo, O. de Q. F., de Medeiros, J. L., A Monte Carlo Methodology for Environmental Assessment Applied to Offshore Processing of Natural Gas with High Carbon Dioxide Content, *J. sustain. dev. energy water environ. syst.*, 8(1), pp 35-55, 2020, DOI: <https://doi.org/10.13044/j.sdewes.d6.0240>

ABSTRACT

Offshore production of oil and natural gas with high carbon dioxide content and high gas-to-oil ratio entail stringent processing conditions that require innovations and first-of-a-kind designs, which bear uncertainties derived from the scarcity of commercial-scale projects, hindering to move along technology learning curves. Consequently, unpredicted scenarios and unachieved specifications cause economic and environmental losses. Such uncertainties force offshore plants to be designed under stochastic factors seeking best statistical performance. The Monte Carlo Method is suitable to such finality. This work proposes a computer-aided engineering framework ‘MCAnalysis’ automatically applying a probabilistic environmental assessment of offshore gas processing. ‘MCAnalysis’ integrates HYSYS simulator with ‘Waste Reduction Algorithm’ to assess potential environmental impacts, whose most relevant categories were identified via Principal Component Analysis. An offshore plant processing natural gas with high carbon dioxide content was submitted to probabilistic raw gas flow rate under two scenarios of carbon dioxide content. The higher carbon dioxide content scenario presented the highest probabilistic potential environmental impacts, being the atmospheric category the most relevant.

KEYWORDS

Environmental assessment, Monte Carlo, Waste reduction algorithm, Principal component analysis, Offshore gas processing, Carbon dioxide rich natural gas.

INTRODUCTION

Offshore Natural Gas (NG) production has been experiencing continuous increase, especially in Brazil, where it is over 36.6 MM Nm³/d [1] as a result of recent discovery of huge oil and gas reserves in deep-water Pre-Salt fields with high Gas-Oil Ratio (GOR) from 250 to 500 Nm³/m³ and high Carbon dioxide (CO₂) content in the associated NG.

* Corresponding author

Exploration and Production of Pre-Salt fields are hence challenged by the environmentally friendly design decision of avoiding NG flaring, requiring large-scale processing of CO₂ rich NG on the topside of Floating Production Storage and Offloading units (FPSO). Processing this stranded NG requires energy intensive operations for CO₂ removal, CO₂ compression and re-injection, and compression of sale gas for export to onshore facilities by subsea pipelines. Additionally to the efficient CO₂ removal, NG processing must include Water Dew Point Adjustment (WDPA) and Hydrocarbon Dew Point Adjustment (HCDPA) to avoid condensation of heavy hydrocarbons and hydrate formation along the pipeline, besides machinery and pipeline for re-injection of CO₂ at very high pressures, creating technology and economic challenges of large magnitude [2].

This scenario requires innovative processes on the topside of FPSO's, resulting in First-Of-A-Kind (FOAK) design conceptions. FOAK technologies bear large uncertainties derived from the absence of prior commercial-scale projects that allow moving along the technology learning curve. Hence, they must be designed considering uncertainties in technologies for CO₂ removal from huge fluxes of CO₂ rich NG, WDPA, and HCDPA, with direct impact on critical variables defining project viability, namely:

- Equipment area and weight;
- NG sale specifications [e.g., Wobbe index, Water Dew-Point (WDP), Hydrocarbon Dew-Point (HCDP) and CO₂ content];
- Energy consumption;
- Economic performance [Capital and Operational Expenditures (CAPEX and OPEX)];
- Environmental performance quantified by several Potential Environment Impact (PEI) categories.

Uncertainties of offshore natural gas processing and Monte Carlo simulations

Many and severe uncertainties affect offshore processing of NG:

- Variability of raw gas composition, pressure and flow rate [3];
- Sales gas price and consumer market, equipment and operational costs [4];
- Meteorological events in high seas and even high operational risks of subsea equipment and topside processes, among others.

Feed composition and flow rate, ambient temperature and pipeline pressure [5] are critical load conditions as their variations propagate effects [6] throughout the plant disturbing operating conditions and product specifications [7]. In industrial practice, uncertainties are usually compensated by the use of conservative decisions like over-design of process equipment and then retrofits to overcome operability bottlenecks, or overestimation of operational parameters caused by worst-case assumptions of uncertain parameters [4], which, despite making the design feasible, drastically decrease profitability [8].

Another relevant uncertainty concerns the impact of the CO₂ re-injection in the reservoir for Enhanced Oil Recovery (EOR). Although EOR increases the efficiency of oil recovery and provides a safe destination for the large volume of CO₂ removed from the NG, it results in a long-term increase of CO₂ content in raw NG. In fact, up to 60% of the re-injected CO₂ can be retained in the reservoir [9], meaning that 40% (or more) stay in the gas phase, rising its CO₂ content, leading to incremental costs and risks throughout the lifetime of offshore NG processing.

Such uncertainties recommend using decision-making techniques under influence of stochastic factors. A classic and powerful technique for decision under non-deterministic scenarios is the Monte Carlo (MC) method. Given advances in computer-aided engineering [10], MC is an adequate technique to estimate the probability of process

designs to accomplish all specification or targets within defined stochastic scenarios of interest. MC method is based on obtaining realizations of the proposed process (responses) under stochastic scenarios randomly sampled according to Probability Density Functions (*PDF*) of the non-deterministic factors that influence process response [11].

Environmental impacts and sustainability assessment of processes

Currently, the process industry is moving towards the design of innovative and more sustainable processes that show improvements in both economic and environmental factors [12]. Corporations worldwide are realizing that sustainability makes good business sense and is fundamental to their survival and growth [13]. Especially, concerns about the impacts of Oil and Gas (O&G) exploitation on the wellbeing of the environment and society have led to increasing pressures for the O&G industry to move towards more sustainable processes [14].

For designing more sustainable processes, besides multiple metrics [15], 'ad hoc' criteria [16] and tools for quantifying sustainability, statistics algorithms for evaluating performance metrics and for supporting decision making have been developed [17]. In the procedure of achieving superior environmental performance, several alternative process flowsheets are generated by combining multiple unit operations, rendering performance assessment of alternatives cumbersome. Therefore, it is beneficial the use of Computer-Aided Engineering (CAE) methods to evaluate all possible alternatives for defining the most sustainable option [12].

The present work

It is presented a CAE tool (MCAnalysis) which automatically integrates the process simulator HYSYS (Aspentech) for obtaining chemical process responses with MATLAB (Mathworks) for generation of graphical statistical analysis using the Waste Reduction (WAR) algorithm (US Environmental Protection Agency) [18] for obtaining statistics of PEI's. In this application, 'MCAnalysis' manages process uncertainties and generates sustainability performance [19] as the result of multiple MC samples of the process responses. 'MCAnalysis' is herein applied to an FPSO plant processing CO₂ rich NG under uncertainties in order to assess the environmental pillar of sustainability, using WAR to evaluate PEI's [20] and PCA to identify the most relevant ones [21]. The assessed process is submitted to probabilistic uncertainties affecting raw NG conditions: flow rate and %mol CO₂, both following normal *PDF*'s. Two scenarios of CO₂ content were compared to evaluate the environmental impact of the increase of %mol CO₂ in raw NG.

This analysis consubstantiates an original work and has potential use for probabilistic sustainability assessments of FPSO gas-oil plants, which are well-known very risky systems operating at very special conditions in terms of safety concerns and exposition to hazards. The developed CAE tool 'MCAnalysis' is also an original achievement as it is reliable, robust and flexible computing resort allowing building several different scenarios of analysis. In the present work, it was configured for environmental assessment of complex offshore gas plant with CO₂ rich NG, but it can also be used for technical, profitability, reliability and safety studies.

METHODS

This section discusses the theoretical aspects and methods pertinent to this work, such as NG processing uncertainties, specification and process design, Monte Carlo method, Waste Reduction Algorithm (WAR), PCA and architecture of the computational tool 'MCAnalysis'.

Offshore processing of carbon dioxide rich natural gas

Offshore processing of raw NG with high CO₂ content is supposed to occur on oil-gas FPSO platforms. Raw NG is first separated from oil and water and then goes to the gas plant at given flow rate, composition, temperature, and pressure. The raw gas is saturated in water (from 2,000 to 3,500 ppm) and its most critical variables are the flow rate and the high content of CO₂. The gas plant is normally designed for a given gas flow rate and CO₂ content, but both variables change along the FPSO campaign, the former because the oil flow rate can change for several reasons at constant GOR, while the latter changes (increases) along the campaign due to continuous injection of CO₂ in the reservoir for EOR. Evidently, several other variables associated with the raw gas can affect the process, but the flow rate and CO₂ content can seriously impact the processing if exceed the design condition. In this work, only the raw gas flow rate and the CO₂ content are considered as relevant process input factors subjected to uncertainties.

Specifications of NG for commercialization. Sales NG is specified in Brazil according to the National Agency of Oil, Gas and Biofuels. The most relevant NG specifications considered in this work are maximum WDP of -45 °C at 1 atm, maximum HCDP of 0 °C at 45 bar, maximum 3%mol CO₂ and minimum 85%mol CH₄.

Gas processing description. The gas plant for offshore processing of CO₂ rich NG is sketched in Figure 1. This process was designed to comply with NG specifications assuming the mean values of critical input factors subjected to uncertainties – flow rate and CO₂ content of the raw gas. This design is denominated as the Base-Case. The objective is to test the Base-Case in terms of environmental impacts via MC sampling. The main operations in the Base-Case (Figure 1) are:

- NG dehydration for WDP;
- Separation of condensable hydrocarbons for HCDPA;
- CO₂ removal.

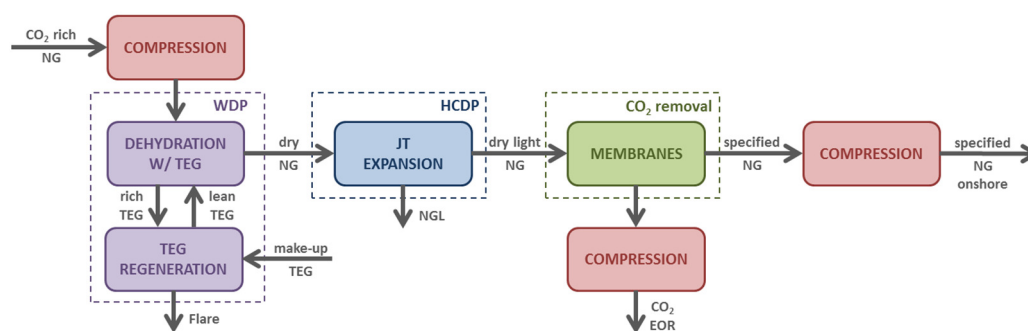


Figure 1. Block diagram of offshore processing of CO₂ rich NG (JT – Joule-Thomson, TEG – Triethylene Glycol, EOR – Enhanced Oil Recovery, WDP – Water Dew Point, HCDP – Hydrocarbon Dew Point, NGL – Natural Gas Liquids)

Triethylene Glycol (TEG) dehydration was chosen for WDP as the most economic option [22], despite requiring a stripping column for TEG regeneration. HCDPA is achieved by Joule-Thomson Expansion (JTE) [23], while CO₂ is removed from NG by Membrane Permeation (MP) due to its operational simplicity, low costs, modularity, capability of processing CO₂ rich feeds, and reduced weight and footprint [24]. The process starts with compression of raw NG, which is sent to TEG dehydration for WDP to avoid ice and gas hydrates in pipelines [25]. Rich TEG is regenerated producing flare gas residue and recirculates to WDP column, while the dry NG flows to HCDPA, where a saleable stream of Natural Gas Liquids (NGL) is a sub-product.

HCDPA must precede MP CO₂ removal to avoid membrane damage by condensable hydrocarbons. In MP CO₂ removal, dry NG flows through a battery of two MP modules, whose outlet MP retentate is the final conditioned NG. Final NG is compressed to be exported to onshore facilities. The MP permeate is a low-pressure CO₂ rich stream which is compressed for re-injection as EOR agent.

Gas processing assumptions for simulation. For each MC realization of the gas plant stochastic input factors, the Base-Case is simulated in HYSYS. The following assumptions are valid for each simulation. {A1} Thermodynamic modelling uses HYSYS Peng-Robinson Package, except for TEG unit with HYSYS Glycol Package. {A2} Reference raw gas composition (%mol) 20% CO₂, 77.88% CH₄, 1.20% C₂H₆, 0.36% C₃H₈, 0.09% iC₄H₁₀, 0.08% C₄H₁₀, 0.04% iC₅H₁₂, 0.02% C₅H₁₂, 0.024% C₆H₁₄, 0.037% C₇H₁₆, 0.024% C₈H₁₈, 0.0023% C₉H₂₀, 0.25% N₂. {A3} Exported NG pressure $P = 250$ bar, {A4} EOR fluid $P = 250$ bar, {A5} Adiabatic efficiencies of compressors and pumps of 75%, {A6} Raw NG compressor with stage compression ratio of 3.525×1 stage, {A7} Exported NG compressor with stage compression ratio of 2.65×2 stages, {A8} CO₂ EOR compressor with stage compression ratio of 3.2×5 stages, {A9} MP using two serial spiral-wound stages of 1.1×10^6 m² and 0.55×10^6 m² of MP area with permeate pressure of 1 bar, temperature difference $T^{\text{RETENTATE}} - T^{\text{PERMEATE}} = 3$ °C and retentate head-loss of 1 bar, {A10} MP simulation via HYSYS Unit Operation Extension MP-UOE from Arinelli *et al.* [26]. {A11} Component permeances (Sm³/d/bar/m²) 6.28 CO₂, 0.314 CH₄, 0.1256 C₂H₆, 0.01256 C₃H₈, 0.01256 iC₄H₁₀, 0.01256 C₄H₁₀, 0.01256 iC₅H₁₂, 0.01256 C₅H₁₂, 0.01256 C₆H₁₄, 0.01256 C₇H₁₆, 0.01256 C₈H₁₈, 0.01256 C₉H₂₀, 0.314 N₂. {A12} Exchangers head-loss of 0.5 bar. {A13} Cooling Water (CW) temperatures: 30 °C and 45 °C at 4 bar. {A14} Pressurized Hot Water (PHW) temperatures: 200 °C and 100 °C at 20 bar. {A15} Gas-liquid thermal approach: 5 °C. {A16} TEG absorber at 70 bar and TEG regenerator at 1.5 bar. {A17} Lean TEG with 0.7%w/w H₂O, rich TEG with 6.6%w/w H₂O. {A18} Gas from intercoolers at 35 °C. {A19} Joule-Thomson Expansion of 64 bar for HCDPA.

Gas plant uncertainties. Uncertainties related to the raw NG were selected for MC analysis. Independent normal random populations were assumed for feed flow rate (MM Sm³/d) and for its CO₂ content as molar fraction because these are the feed factors with the highest influence on the process response and also with the highest subsection to uncertainties. Normal *PDF*'s were chosen due to their relevance for describing multiple physical, meteorological, biological and financial phenomena. One can argue that normal *PDF*'s are not adequate to represent real stochastic disturbances because they have infinite tails spread on $(-\infty, +\infty)$ domains, whereas the reality is not akin to infinite amplitude inputs. Well, this is not the case. First of all, there are, indeed, (very) rare natural events with relatively gigantic catastrophic amplitudes (someone does not have to be especially imaginative to cite one). Secondly, the 99.73% probability domain of normal *PDF*'s corresponds to the finite interval $[\mu - 3\sigma, \mu + 3\sigma]$, while the 99.99% probability domain corresponds to $[\mu - 4\sigma, \mu + 4\sigma]$, where μ and σ are, respectively, the population mean and standard deviation. This implies that more than 10,000 outcomes have to be sampled to have a single one outside the $[\mu - 4\sigma, \mu + 4\sigma]$ interval, while MC searches are applied with finite samples containing from 1,000 to 3,000 outcomes, which is sufficient for ergodicity [27]. In other words, on practical grounds normal *PDF*'s give rise to bounded unimodal samples. Other advantages of normal *PDF*'s are:

- By the Central Limit Theorem a normal input is appropriate to represent the contribution of several other independent inputs following arbitrary distributions (which is, in real applications, the case of some unimodal disturbances that represent a collection of contributions);

- Normal *PDF*'s may degenerate to other simpler *PDF*'s like the Dirac *PDF*.

Additionally, there is a very special reason to adopt normally distributed input factors. This has to do with the traceability of normal signals throughout the process. When submitted to uncertainties following normal *PDF*'s, process output variables shall present behaviours close to the normal pattern for approximately linear cause-effect relationships, whereas behaviours very different from normal (e.g. bimodal, multi-modal or stone-wall responses) would be observed for very non-linear causality relationships. In other words, using normal inputs one can identify where there is great non-linearity in the process response. This may be useful in sensitivity studies, design of process control strategies and when applying design safe margins to some critical process units. The normal *PDF* of variable x is given by eq. (1) with its parameters μ (mean) and σ (standard deviation). In the present case, the raw NG flow rate population is supposed to follow a normal *PDF* with $\mu = 6.0 \text{ MM Sm}^3/\text{d}$ and $\sigma = 1 \text{ MM Sm}^3/\text{d}$, meaning that it practically varies from 3.0 to 9.0 $\text{MM Sm}^3/\text{d}$. Meanwhile, two scenarios were devised for the CO_2 content populations of raw NG: Case 20% – using normal *PDF* with $\mu = 0.20$ and $\sigma = 0.03$ (i.e. CO_2 molar fraction approximately varies from 0.10 to 0.30), and Case 50% – using normal *PDF* with $\mu = 0.50$ and $\sigma = 0.03$ (i.e. CO_2 molar fraction approximately varies from 0.40 to 0.60), as shown in Figure 2.

$$PDF(x, \mu, \sigma) = \frac{1}{\sqrt{2\pi\sigma^2}} e^{-\frac{(x-\mu)^2}{2\sigma^2}}, -\infty < x < \infty, \sigma > 0 \quad (1)$$

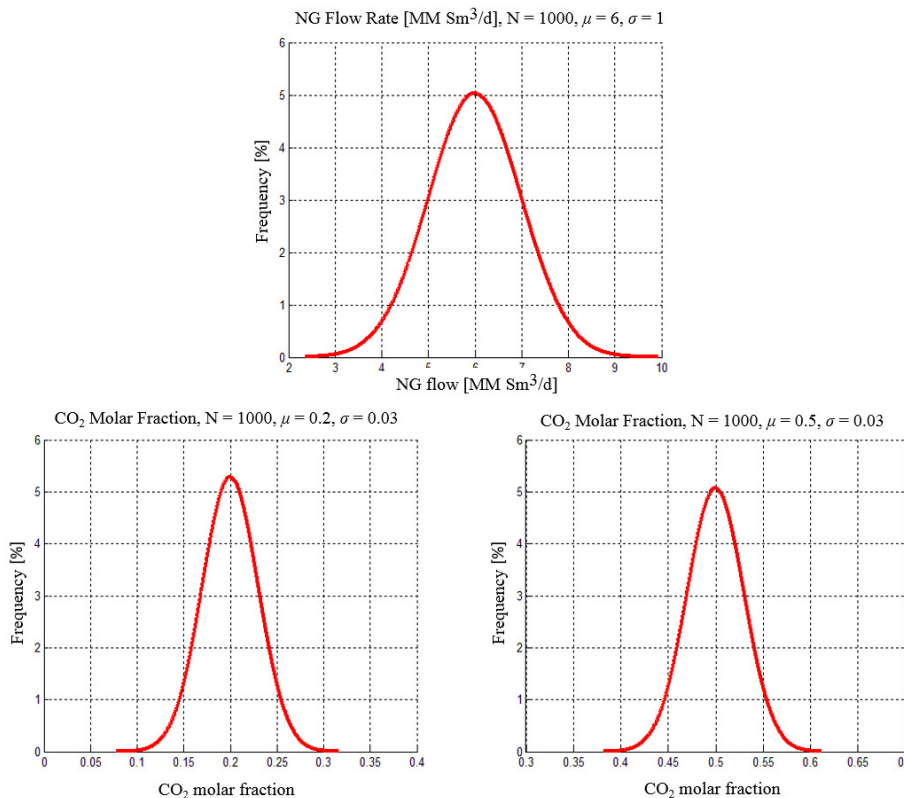


Figure 2. *PDF*'s of: raw NG flow rate population [$\text{MM Sm}^3/\text{d}$] (a), feed NG CO_2 molar fractions populations for: Case 20% CO_2 (b) and Case 50% CO_2 (c)

Monte Carlo sampling

MC is a relevant methodology based on stochastic analysis for evaluating systems under non-deterministic scenarios when analytical solutions are complex or impossible due to non-deterministic components which are not known *a priori* [11]. Such

methodology provides an approximation of the problem solution by stochastic sampling of the independent system variables obeying known *PDF* instead of solving the numeric-mathematical problem directly. The objective of MC analysis is the stochastic appraisal of the performance of a given dependent variable of interest (output variable) according to the behaviour of uncertain independent variables (input variables). The method consists on creating samplings of the independent variables by generating pseudo-random numbers distributed between 0 and 1 which are converted to random samples obeying *PDF*'s of the independent variables, given that the behaviour of these independent variables is random and follows specific *PDF*'s. When a large sample of random values of independent variables is used, the calculated values of output variables can be plotted as histograms, leading to approximations of *PDF*'s of output variables, which are the main objectives of MC analysis jointly with some statistics for estimating parameters of these *PDF*'s (e.g. sample mean and sample standard deviation).

This work uses the Inverse Transform Method [28] to generate normal pseudo-random populations. This method employs random number properties and the Cumulative Distribution Function (*CDF*) of a random variable to generate its sample *PDF*. The correlation of a random number with the *CDF* is given by eq. (2), which can be inverted to generate eq. (3) based on the *iCDF* (inverse of *CDF*) for expressing the mapping of a set of values of the variable of interest from a set of random values uniformly distributed between 0 and 1:

$$\int_a^{x1} PDF(x)dx = CDF(x1) = CDF(rnd1) = \int_0^{rnd1} PDF(rnd)d(rnd) = rnd1 \quad (2)$$

$$x1 = iCDF(rnd1) \quad (3)$$

where *rnd* is a random number uniformly distributed between 0 and 1, *rnd1* is a sample of *rnd* between 0 and 1, *x* is another random number varying along the domain $a \leq x \leq b$, *x1* is a sample of *x* between *a* and *b*, *PDF*(*rnd*) and *PDF*(*x*) are the *PDF*'s of variables *rnd* and *x*, and *CDF*(*rnd*) and *CDF*(*x*) the integrals of *PDF*(*rnd*) and *PDF*(*x*).

The *iCDF* – inverse of the *CDF* – for the standard normal distribution ($\mu = 0, \sigma = 1$) is numerically approximated in eq. (4) and eq. (5) [29]. Eq. (4) and eq. (5) correspond to the conversion of a population of pseudo-random numbers sampled from 0 to 1 into a population following the standard normal *PDF* with an absolute error smaller than 4.5×10^{-4} , where $c_0 = 2.515517, c_1 = 0.8202853, c_2 = 0.010328, d_1 = 1.432788, d_2 = 0.189269$ and $d_3 = 0.001308$. The symmetry of normal *PDF* is considered so that eq. (4) and eq. (5) are valid for $0 < p \leq 0.5$. For $0.5 < p \leq 1$, eq. (4) and eq. (5) are used with $1 - p$, switching the signal of the calculated abscissa *z*. With eq. (4) and eq. (5) the population of *z* values generated from the population of *p* values approximately follows the standard normal *PDF*. Eq. (6) converts the population of standard normal *z* to a normal population *x* with mean μ and standard deviation σ . Figure 3 depicts the relationships between samples via *iCDF* and *CDF* to generate samples according to normal *PDF*'s:

$$t = \sqrt{-2 \ln p} \quad (4)$$

$$z_p = t - \frac{c_0 + c_1 t + c_2 t^2}{1 + d_1 t + d_2 t^2 + d_3 t^3} \quad (5)$$

$$z = \frac{(x - \mu)}{\sigma} \rightarrow x = \mu + z \times \sigma \quad (6)$$

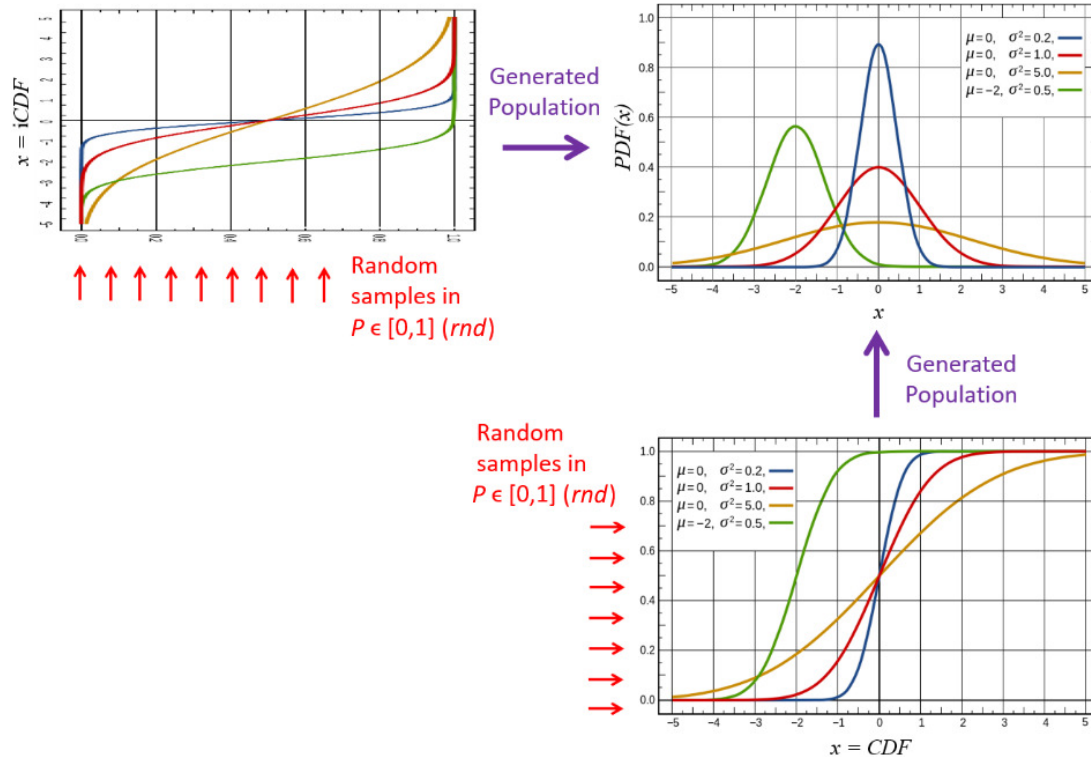


Figure 3. Interrelationships among iCDF, CDF, and PDF of normal populations

Quasi-Monte Carlo sampling versus Monte Carlo sampling

The Quasi-MC (Quasi Monte Carlo) is an alternative sampling method for multi-dimensional numerical integrations and similar contexts where conventional MC sampling is applied. Quasi-MC uses low-discrepancy sequences – such as, the Halton and Sobol sequences – also called quasi-random or sub-random sequences [30]. Quasi-MC is presented in opposition to the regular MC sampling applications such as multi-dimensional MC integrations, which are based on pseudo-random sequences. MC and Quasi-MC samplings are adequate for multi-dimensional integrations where common numerical strategies – such as Newton-Cotes quadrature formulas – face severe difficulties. The advantage of Quasi-MC is its faster rate of convergence [$O(1/N)$] relatively to regular MC [$O(1/\sqrt{N})$], where N is the number of samples. On the other hand, Quasi-MC has some drawbacks comparatively to MC [31], such as:

- Its superiority over MC only appears if N is really high and the dimensionality (number of independent factors) is not too high;
- A majoring of the involved Quasi-MC error sometimes cannot be found for very non-linear response functions – e.g. multi-modal responses;
- Regular MC is very easy to implement even for very non-linear response functions as in the present case with offshore gas plants processing CO₂ rich NG;
- The high non-linear behaviour of some response functions may bring multi-modal responses for unimodal inputs (e.g. with normal PDF's) – as shown in the present study in Figures 9-15 – such that the higher performance of Quasi-MC may be hampered by such patterns, vis-à-vis the resiliency of regular MC in such cases.

Despite the apparent superiority of Quasi-MC over MC, in the present work, only regular MC sampling is used. The main reason has to do with the much easier and robust implementation of MC sampling in the environment of 'MCAnalysis' juxtaposed to the fact that the number of flowsheet simulations is not too high for statistical convergence of the sample mean and variance of responses – from 1,000 to 2,000 simulations are normally required with two stochastic input factors – and also the fact that the real

time-consuming step is the simulation of the complex gas plant (i.e. evaluation of the process response) and not the sampling management algorithm itself.

Environmental performance of processes – Waste Reduction algorithm

Several methodologies for characterizing the environmental impact of products and processes are available in the literature, as Life Cycle Assessment (LCA) and Waste Reduction (WAR), both well-established techniques to include environmental considerations into process design [32]. The LCA methodology assesses the environmental performance of a product or process thorough its life cycle: from the primary resources to recycling or safe disposal [33]. However, this methodology requires a large amount of information and few data are publicly available due to legal or intellectual property concerns [34]. The WAR methodology considers only the product manufacturing step [19] as Figure 4 shows. WAR is selected to be used in this work due to its simplicity when compared to LCA. It is worth noting that WAR, contrarily to LCA, is restricted to ‘gate-to-gate’ analysis (Figure 4).

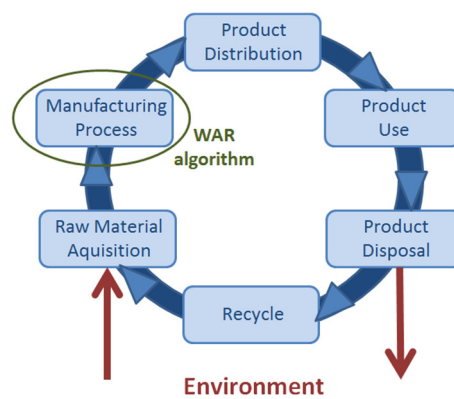


Figure 4. WAR algorithm with plant life cycle (adapted from [19])

WAR was proposed by Cabezas *et al.* [18] as a general theory for the flow and generation of PEI’s through a chemical process and is used to quantify its environmental performance. By definition, PEI is the unrealized average effect or impact that the emission of mass and energy would cause to the environment, being essentially a probability function associated to a potential effect. A PEI conservation equation based on an accounting of the flow of PEI in/out of the product manufacturer and energy

generation [20], is introduced by WAR in eq. (7) for steady state balance, where $\dot{I}_{in}^{(cp)}$ and $\dot{I}_{out}^{(cp)}$ are the input and output rates of PEI of the chemical process, $\dot{I}_{in}^{(ep)}$ and $\dot{I}_{out}^{(ep)}$ are the input and output rates of PEI of the energy generation process, $\dot{I}_{we}^{(cp)}$ and $\dot{I}_{we}^{(ep)}$ are the output of PEI associated with the waste energy lost from the chemical and energy generation processes and $\dot{I}_{gen}^{(t)}$ represents the creation or consumption of PEI by chemical reactions inside the chemical process and the power plant. Figure 5 illustrates eq. (7):

$$\dot{I}_{in}^{(cp)} + \dot{I}_{in}^{(ep)} - \dot{I}_{out}^{(cp)} - \dot{I}_{out}^{(ep)} - \dot{I}_{we}^{(cp)} - \dot{I}_{we}^{(ep)} + \dot{I}_{gen}^{(t)} = 0 \tag{7}$$

PEI is calculated by a unified score obtained by the weighted sum of eight environmental impact categories, listed in Table 1, and a specific PEI for each impact category is associated to the components of the process streams as shown in eq. (8), where l is an indicator for input or output, α_i is the weighting factor for environmental

impact category i , $\dot{M}_{j,l}$ is the mass flow of stream j , x_{kj} is the mass fraction of component k in stream j and ψ_{ki}^s is the specific PEI of component k associated with environmental impact category i . The measures for calculating each ψ_{ki}^s are also listed in Table 1. The calculation of ψ_{ki}^s is given by eq. (9) where $(\text{Score})_{ki}$ represents the impact score of component k correlated with environmental category i and $\langle(\text{Score})_k\rangle_i$ represent the average impact score of all components in category i . This normalization of the component impact eliminates unnecessary bias within the category. The specific correlations among each category score and its corresponding measure of impact are described in Young and Cabezas [19]. The environmental assessment in this work presents the output PEI's for each individual category caused by the offshore processing of CO₂ rich NG and identifies the most relevant as performance indicators using PCA. Impacts from product streams are not considered.

$$\dot{I}_l = \sum_i^{\text{EnvCats}} \alpha_i \sum_j^{\text{Streams}} \dot{M}_{j,l} \sum_k^{\text{Comps}} x_{kj} \psi_{ki}^s \quad (8)$$

$$\psi_{ki}^s = \frac{(\text{Score})_{ki}}{\langle(\text{Score})_k\rangle_i} \quad (9)$$

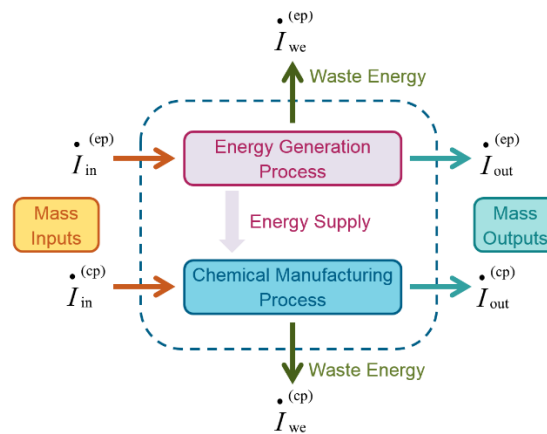


Figure 5. WAR algorithm (adapted from [20])

Table 1. PEI categories and measure of impact associated with PEI category [35]

General PEI category	PEI category	Measure of impact of PEI category
Human toxicity	Ingestion (HTPI)	LD ₅₀
	Inhalation/dermal (HTPE)	OSHA PEL
Ecological toxicity	Aquatic Toxicity (ATP)	Fathead Minnow LC ₅₀
	Terrestrial Toxicity (TTP)	LD ₅₀
Global atmospheric impacts	Global Warming Potential (GWP)	GWP
	Ozone Depletion Potential (ODP)	ODP
Regional atmospheric impacts	Acidification Potential (AP)	AP
	Photochemical Oxidation Potential (PCOP)	PCOP

Principal Component Analysis

Principal Component Analysis (PCA) consists in re-organizing data sets (e.g. data from process plants), which often exhibit correlated patterns, in order to find a set of new uncorrelated variables as linear combination of the original ones. The new variables are assigned to fractions of the variance in the original data in decreasing order [21].

The original data set is organized as a matrix $\underline{\underline{X}}_{m \times n}$, where the scalar variables of the problem correspond to the columns and their samples correspond to the rows, meaning that each vector of sampled data \underline{X}_i for variable X_i corresponds to a column of the matrix $\underline{\underline{X}}$, as illustrated by eq. (10). Each vector \underline{X}_i originates a sample scalar mean $\langle X_i \rangle$ given by eq. (11). Such sample means are gathered in the vector of means $\langle \underline{X} \rangle$ as shown in eq. (12). $\underline{U}_{m \times 1}$ is a compatible vector of ones:

$$\begin{array}{cccc} X_1 & X_2 & \dots & X_n \\ \downarrow & \downarrow & \dots & \downarrow \\ \begin{bmatrix} x_{11} & x_{12} & \dots & x_{1n} \\ x_{21} & x_{22} & \dots & x_{2n} \\ \dots & \dots & \dots & \dots \\ x_{m1} & x_{m2} & \dots & x_{mn} \end{bmatrix} & = & [\underline{X}_1 \ \underline{X}_2 \ \dots \ \underline{X}_n]; & \underline{X}_1 = \begin{bmatrix} x_{11} \\ x_{21} \\ \dots \\ x_{m1} \end{bmatrix}; & \underline{X}_2 = \begin{bmatrix} x_{21} \\ x_{22} \\ \dots \\ x_{m2} \end{bmatrix}; & \underline{X}_n = \begin{bmatrix} x_{1n} \\ x_{2n} \\ \dots \\ x_{mn} \end{bmatrix} \end{array} \quad (10)$$

$$\langle X_i \rangle = \underline{U}^T \underline{X}_i / m \quad (11)$$

$$\langle \underline{X} \rangle = [\langle X_1 \rangle \ \dots \ \langle X_n \rangle]^T \quad (12)$$

PCA factorizes the matrix of sample variance-covariance $\underline{\underline{R}}_{X \ n \times n}$ – symmetric and positive definite – obtained by eq. (13). The n eigenvalues of $\underline{\underline{R}}_{X}$ are calculated and expressed as a column vector of positive eigenvalues $\underline{\lambda}$ sorted in decreasing order, while the respective orthogonal normalized n eigenvectors ($n \times 1$) are stored as columns of matrix $\underline{\underline{P}}$ as illustrated in eq. (14):

$$\underline{\underline{R}}_{X} = \frac{(\underline{\underline{X}} - \underline{U} \cdot \langle \underline{X} \rangle^T)^T (\underline{\underline{X}} - \underline{U} \cdot \langle \underline{X} \rangle^T)}{m-1} \quad (13)$$

$$\underline{\lambda} = \begin{bmatrix} \lambda_1 \\ \vdots \\ \lambda_n \end{bmatrix}, \quad \underline{\underline{P}} = [\underline{P}_1 \ \dots \ \underline{P}_n] \quad (14)$$

Matrix $\underline{\underline{P}}$ contains the directions capable of describing the variability of original data $\underline{\underline{X}}$ by decreasing relevance, meaning that $\underline{\underline{X}}$ data show more variability over the direction defined by the first column of $\underline{\underline{P}}$. This is the 1st principal direction for describing the statistical behaviour of $\underline{\underline{X}}$. The second column of $\underline{\underline{P}}$ is the 2nd principal direction and so on. A matrix of generalized scores $\underline{\underline{S}}_{m \times n}$ is obtained by projecting $\underline{\underline{X}}$ over the directions (columns) of $\underline{\underline{P}}$ after subtracting the respective sample means $\langle X_i \rangle$ as eq. (15) shows, where \underline{P}_i is the principal direction i of $\underline{\underline{P}}$ and \underline{S}_i contains $m \times 1$ samples of the generalized score S_i . The generalized scores are the new scalar variables S_1, S_2, \dots, S_n candidates to substitute the original variables X_1, X_2, \dots, X_n with the advantage of having the variability condensed to its maximum and decreasing along the elements of the set. Usually, the first elements represent most of the variability of the original set. The percentage of the variance associated to the general score S_i is calculated considering its contribution over the total variance of the sample as shown in eq. (16):

$$\underline{S}_i = (\underline{X} - \underline{U} < \underline{X}^T >) \underline{P}_i \quad (15)$$

$$v_i [\%] = 100 \frac{\lambda_i}{\sum_i \lambda_i} \quad (16)$$

Software ‘MCAnalysis’

In order to enable the automatic execution of MC analysis for any chemical process representable as a simulation flowsheet, a set of random sample values of the process input stochastic variables must be generated, managed and submitted to process simulation to generate output samples which are then statistically processed to generated statistics results and figures. Therefore ‘MCAnalysis’ was designed as a HUB to manage MC analysis for several different scenarios of stochastic response like technical analysis of a process design, safety analysis, energy consumption assessment, economic assessments and environmental sustainability assessment (Figure 6). In this work only the environmental assessment is demonstrated.

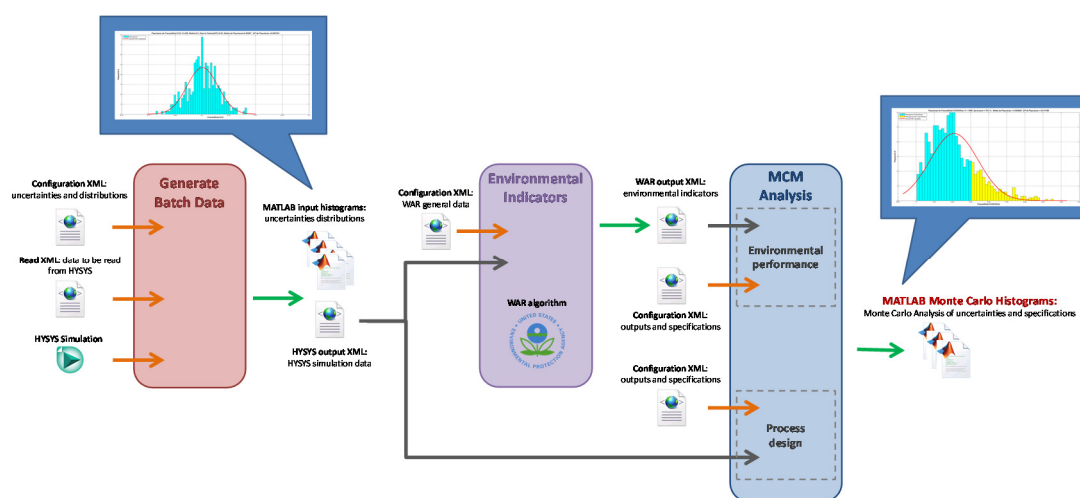


Figure 6. HUB architecture of ‘MCAnalysis’

‘MCAnalysis’ starts with the module “Generate Batch Data”, which processes a configurable XML (Configuration XML) containing the definition of the MC non-deterministic independent input variables, the respective *PDF*’s and how to identify them in the HYSYS simulation flowsheet. Populations of the input stochastic variables are randomly generated and graphically processed through MATLAB for generating histograms and plotting associated *PDF* curves. HYSYS simulation is then executed in batch for each sample of the input variables. The relevant simulated responses for the MC analysis, listed in another configuration XML (Read XML), are gathered and stored in an output XML file (HYSYS output XML). The batch data generated from the simulation can then be used for process design or assessment of environmental performance with MC analysis.

For technical analysis of a process design, HYSYS output XML is processed by the module ‘MCM Analysis’ together with a configurable XML (Configuration XML) containing the output variables relevant for MC analysis as well as their maximum or minimum specifications (if the variable is a design specification) for graphical presentation of MC analysis results through MATLAB: histograms, *PDF* curves and percentage of success achieved by the sampled cases. As for environmental performance assessment, HYSYS output XML is processed by the module ‘Environmental Indicators’ together with a configurable XML (WAR general data), which is extracted from HYSYS

with components, input and output streams, where the output streams are classified by the user as product or waste. This module uses the WAR algorithm data [35] to generate an XML (WAR output) containing PEI's classified according to the eight environmental impact categories for all the samples of MC analysis. For the environmental performance assessment itself, this output XML is processed by the module 'MCM Analysis' in the same way as the HYSYS output XML.

RESULTS AND DISCUSSIONS: ENVIRONMENTAL ASSESSMENT VIA MONTE CARLO ANALYSIS

The environmental performance was assessed for the process design with two mean CO₂ contents in the raw gas feed: Case 20% CO₂ and Case 50% CO₂. The respective flowsheets of both cases were previously designed with MC analysis in order to achieve a minimum of 75% success frequency for all design specifications in the sampled cases. Populations of 1,000 random samples for each independent stochastic input were used. Specifications WDP, HCDP and minimum molar fraction of methane were achieved with success in 100% of the samplings for both cases. Maximum 3%mol fraction of CO₂ in the exported NG was reached in 83.3% of the samples for Case 20% CO₂ and in 82.1% for Case 50% CO₂. Figure 7 shows histograms and *PDF* curves of the sampled populations of the input variables. The amount of sampled cases, sample mean μ and sample standard deviation σ of the populations as well as their theoretical and expected values, are available in the title bar of each graphic. In all graphical results in this study, the similarity of the response behaviour with a normal pattern is tested by depicting the population histograms with the corresponding normal *PDF* using the sample mean and standard deviation as parameters. For example, Figure 7 confirms for the two stochastic input factors – flow rate and CO₂ content of raw gas – the similarity of sampled and theoretical population parameters, and the similarity of population histograms and normal *PDF* curves. These numerical and graphical similarities attest that the sampling was successful in terms of reproducing the respective normal behaviours.

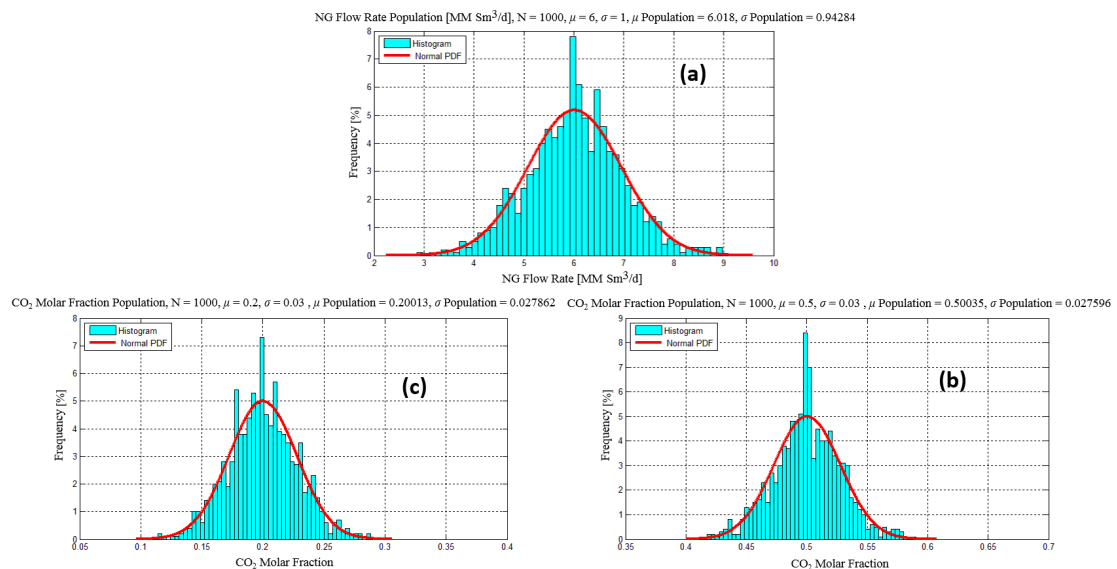


Figure 7. Histograms and comparative normal *PDF*'s of: raw NG flow rate population [MM Sm³/d] (a), raw NG CO₂ molar fraction populations for: raw NG with 20%mol CO₂ (b) and raw NG with 50%mol CO₂ (c)

After designed under uncertainties with MC analysis, the gas plant flowsheets adequate to Case 20% CO₂ and Case 50% CO₂ were submitted to environmental assessment with MC analysis. The intent is to disclose the behaviour of the

environmental indicators in Table 1 for the gas plant operating under stochastic inputs. The results are shown in Figures 8-15 which depict histograms and normal *PDF*'s for populations of output PEI's from the eight environmental impact categories considered in WAR algorithm (Table 1). The normal *PDF*'s built with sample mean and sample standard deviation serve as qualitative indications of the suitability of normal patterns to represent the statistical behaviour of the corresponding MC responses. The number of samples, percentage of samples which attained or exceeded specifications, sample mean μ and sample standard deviation σ are available in the title bar of each graphic.

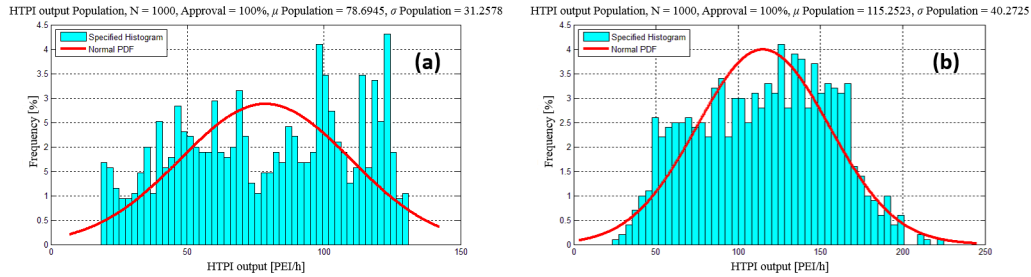


Figure 8. Histograms and Normal *PDF*'s of output HTPI [PEI/h] for: Case 20% CO₂ (a) and Case 50% CO₂ (b)

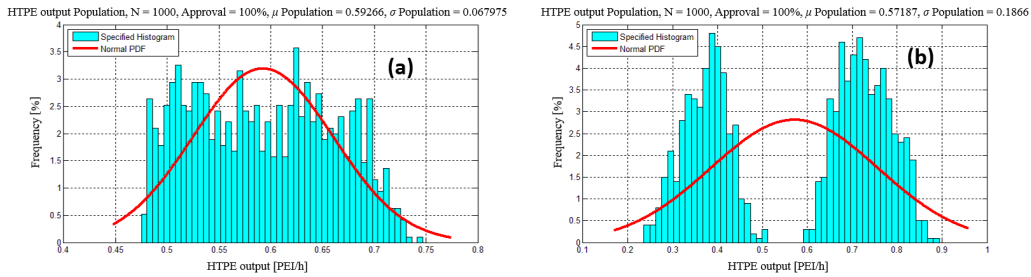


Figure 9. Histograms and Normal *PDF*'s of output HTPE [PEI/h] for: Case 20% CO₂ (a) and Case 50% CO₂ (b)

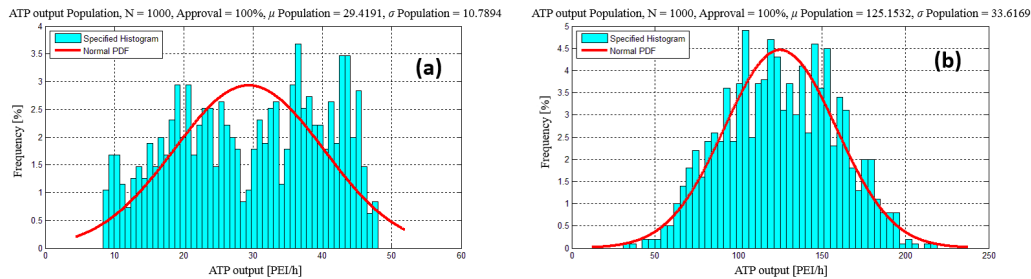


Figure 10. Histograms and Normal *PDF*'s of output ATP [PEI/h] for: Case 20% CO₂ (a) and Case 50% CO₂ (b)

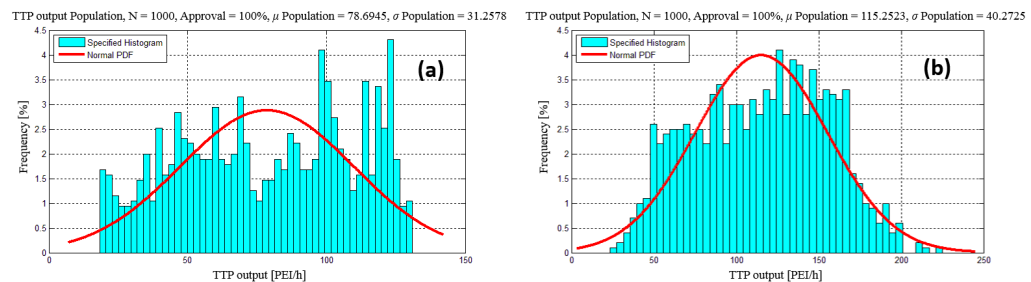


Figure 11. Histograms and Normal *PDF*'s of output TTP [PEI/h] for: Case 20% CO₂ (a) and Case 50% CO₂ (b)

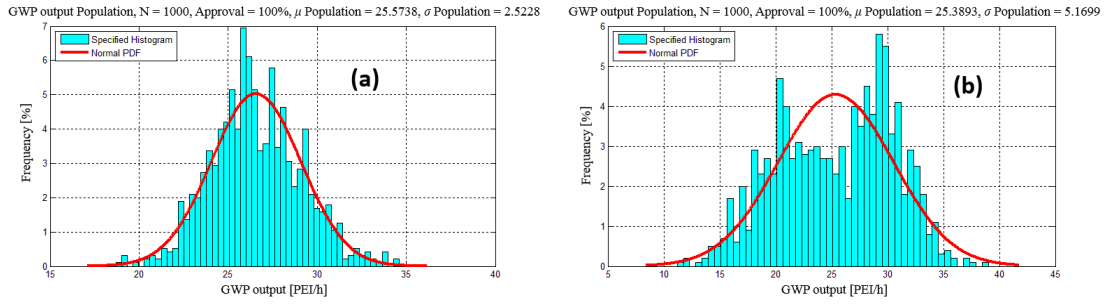


Figure 12. Histograms and Normal *PDF*'s of output GWP [PEI/h] for: Case 20% CO₂ (a) and Case 50% CO₂ (b)

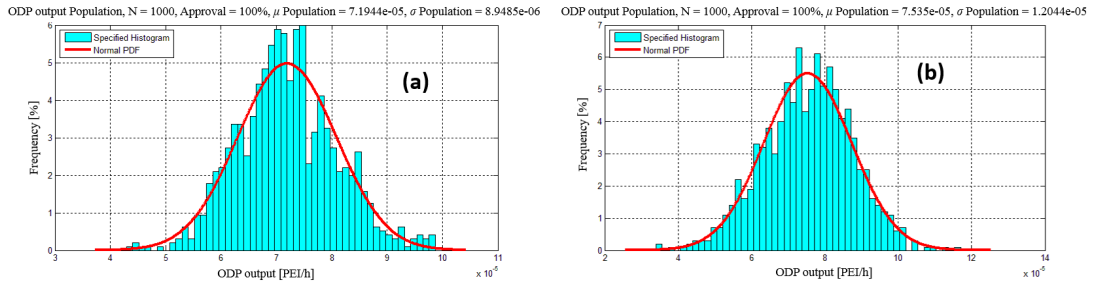


Figure 13. Histograms and Normal *PDF*'s of output ODP [PEI/h] for: Case 20% CO₂ (a) and Case 50% CO₂ (b)

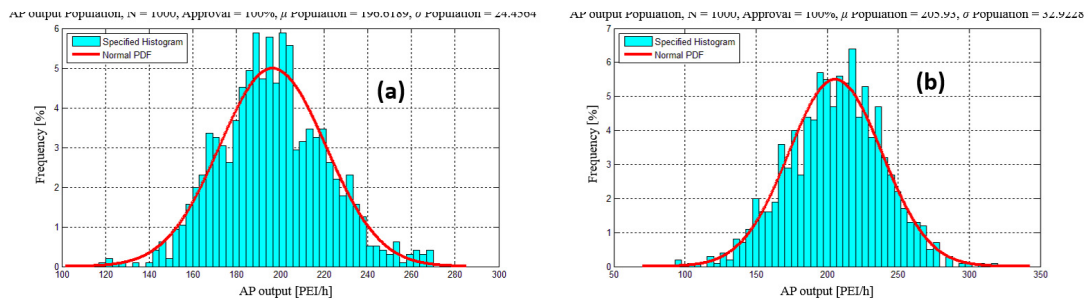


Figure 14. Histograms and Normal *PDF*'s of output AP [PEI/h] for: Case 20% CO₂ (a) and Case 50% CO₂ (b)

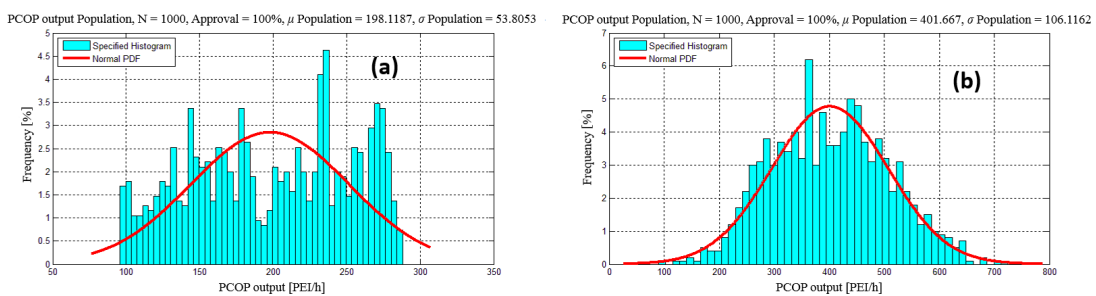


Figure 15. Histograms and Normal *PDF*'s of output PCOP [PEI/h] for: Case 20% CO₂ (a) and Case 50% CO₂ (b)

When considering the uncertainties of both feed gas flow rate and CO₂ molar fraction, the histograms of HTPI, HTPE, TTP for both cases, ATP and PCOP for Case 20% CO₂ and GWP for Case 50% CO₂ presented behaviour completely different from normal *PDF*, which shows that the process responds to uncertainties in a highly non-linear way regarding environmental performance. In each one of these instances, the impertinence of normal behaviour can be visualized by means of the discrepancy between the statistical

behaviour of the histogram and the respective normal *PDF* built with sample mean and sample standard deviation from the histogram. The remaining PEI's presented behaviour relatively close to normal patterns. In addition, the histograms of HTPI, HTPE, ATP, TTP, GWP and PCOP exhibit some difference of patterns for the 20% and 50% CO₂ content cases. This means that the process responds non-linearly to changes in the CO₂ content of raw NG regarding most of the environmental indicators. Table 2 summarizes the percent differences between sample mean μ and sample standard deviation σ between the populations for the two CO₂ content cases relative to the values of Case 20% CO₂.

Table 2. Summary of output PEI categories, sample mean μ and sample standard deviation σ for Cases 20% CO₂ and 50% CO₂

Output PEI category	Sample μ [PEI/h] Case 20% CO ₂	Sample μ [PEI/h] Case 50% CO ₂	Difference [%]	Sample σ [PEI/h] Case 20% CO ₂	Sample σ [PEI/h] Case 50% CO ₂	Difference [%]
HTPI	78.6954	115.2523	46	31.2578	40.2725	29
HTPE	0.5927	0.5719	-4	0.0680	0.1866	175
ATP	29.4191	125.1532	325	10.7894	33.6199	212
TTP	78.6945	115.2523	46	31.2578	40.2725	29
GWP	26.5738	25.3893	-4	2.5228	5.1699	105
ODP	7.19E-05	7.54E-05	5	8.95E-06	1.20E-06	-87
AP	196.6189	205.9300	5	24.4564	32.9228	35
PCOP	198.1187	401.6670	103	53.8053	106.1162	97

By assigning equal weights to each environmental category, the total output PEI is depicted in Figure 16, showing that the Case 50% CO₂ has a sample mean 62% higher than Case 20% CO₂ and sample standard deviation 74% higher. Therefore, the long-term increase of CO₂ content in raw NG caused by CO₂ reinjection due to EOR will deteriorate the environmental performance of the process.

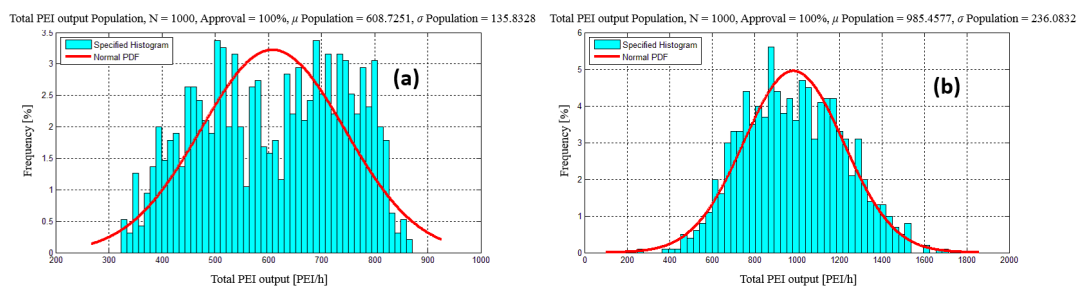


Figure 16. Histograms and Normal *PDF*'s of total output PEI [PEI/h] for: Case 20% CO₂ (a) and Case 50% CO₂ (b)

In addition, the most relevant environmental impact categories were identified with PCA. Table 3 shows the eigenvalues (λ_i), the variances (v_i) and the cumulative variances for Case 20% CO₂ and Case 50% CO₂. It can be concluded that the first two principal components PC(1) and PC(2) are the only relevant components for explaining the environmental performance of the process, corresponding to, respectively, 81.2% and 18.8% of the variance of Case 20% CO₂ and to 92.6% and 6.5 of Case 20% CO₂. For identifying the dominant environmental impact categories corresponding to PC(1) and PC(2), the components of vectors \underline{P}_i with higher absolute values listed in Table 4 for Case 20% CO₂ and Case 50% CO₂, correspond to the most relevant categories.

Table 4 shows that the environmental impact categories GWP (global atmospheric impacts), AP and PCOP (regional atmospheric impacts) are the most significant to PC(1), having high relevance to the process for both cases. When PC(2) is also included, the environmental impact category TTP (ecological toxicity) can be considered as medium relevance to the process for both cases.

Table 3. Eigenvalues λ_i and variance v_i for each principal component for Case 20% CO₂ and Case 50% CO₂

Case 20% CO ₂								
Principal component	PC(1)	PC(2)	PC(3)	PC(4)	PC(5)	PC(6)	PC(7)	PC(8)
λ_i	4,994.8	574.7718	0.3601	0.0364	0.0024	0	0	0
v_i [%]	89.6738	10.3191	0.0065	0.0007	0	0	0	0
Cumulative variance [%]	89.6738	99.9928	99.9993	100	100	100	100	100
Case 50% CO ₂								
Principal component	PC(1)	PC(2)	PC(3)	PC(4)	PC(5)	PC(6)	PC(7)	PC(8)
λ_i	11,551	1,083.3	145.4925	6.7193	0.0199	0	0	0
v_i [%]	92.6247	6.4694	0.08689	0.0369	0.0001	0	0	0
Cumulative variance [%]	92.6247	99.0941	99.963	99.9999	100	100	100	100

Table 4. \underline{P}_i vector of each principal component: Cases 20% CO₂ and 50% CO₂

Case 20% CO ₂								
\underline{P}_i	PC(1)	PC(2)	PC(3)	PC(4)	PC(5)	PC(6)	PC(7)	PC(8)
HTPI	0.0158	0.0940	0.2728	-0.4001	0.8689	-0.0373	-0.0000	-0.0000
HTPE	0.1526	0.0022	-0.4869	0.7134	0.4795	0.0285	-0.0000	-0.0000
ATP	0.0009	-0.0000	0.0247	-0.3557	0.0186	0.9989	0.0000	-0.0000
TTP	0.0806	0.9920	-0.0290	0.0205	-0.0901	0.0031	-0.0000	-0.0000
GWP	0.4420	-0.0441	-0.4182	-0.3557	-0.0358	-0.0021	0.0000	-0.7071
ODP	0.00000	0.0000	-0.0000	-0.0000	0.0000	-0.0000	1.0000	0.0000
AP	0.4420	-0.0441	-0.4182	-0.3557	-0.0358	-0.0021	0.0000	0.7071
PCOP	0.7611	-0.0563	0.5808	0.2763	-0.0631	-0.0040	0.0000	-0.0000
Case 50% CO ₂								
\underline{P}_i	PC(1)	PC(2)	PC(3)	PC(4)	PC(5)	PC(6)	PC(7)	PC(8)
HTPI	0.0138	0.0940	0.2728	-0.4001	0.8689	-0.0373	-0.0000	-0.0000
HTPE	0.2608	0.0022	-0.4869	0.7134	0.4795	0.0285	-0.0000	-0.0000
ATP	0.0005	-0.0000	0.0247	-0.3557	0.0186	0.9989	0.0000	-0.0000
TTP	0.0806	0.9920	-0.0290	0.0205	-0.0901	0.0031	-0.0000	-0.0000
GWP	0.3133	-0.0441	-0.4182	-0.3557	-0.0358	-0.0021	0.0000	-0.7071
ODP	0.0000	0.0000	-0.0000	-0.0000	0.0000	-0.0000	1.0000	0.0000
AP	0.3133	-0.0441	-0.4182	-0.3557	-0.0358	-0.0021	0.0000	0.7071
PCOP	0.7611	-0.0563	0.5808	0.2763	-0.0631	-0.0040	0.0000	-0.0000

CONCLUSIONS

MC analysis was successfully applied for environmental assessment of offshore processing of CO₂ rich NG considering uncertainties on raw NG flow rate and CO₂ content. Processing NG with higher CO₂ content carries a higher potential environmental impact, as expected, since CO₂ is the main emission from the plant, due to the power demand of compressors for NG exportation and CO₂ injection for EOR. This result raises an alert for the impact of the CO₂ injection in the reservoir for EOR, which will increase the CO₂ content in the NG in the long-term.

The statistical behaviours of the PEI's corresponding to each environmental potential category evidence highly non-linear responses of the process, which validates the

recommendation to adopt decision making under influence of stochastic factors as MC analysis. Furthermore, the CAE tool ‘MCAnalysis’ was shown to be valuable for this kind of analysis, as it can handle uncertainties affecting process responses for a given design and address sustainability performance of the process.

The categories GWP (global atmospheric impacts), AP and PCOP (regional atmospheric impacts) were identified by PCA as very relevant to process environmental performance under uncertainties, while the category TTP (ecological toxicity) exhibited medium relevance, independently of the CO₂ content of raw NG, because TTP is also related to emissions of unburnt hydrocarbons in the atmosphere due to leakages and incomplete burning. These aspects have reflexes on FPSO design decision-making and can influence environmental policies of regulating agencies in connection with CO₂ rich NG exploration and production by offshore platforms.

ACKNOWLEDGMENT

Authors are indebted to Dr. Heriberto Cabezas, Dr. Douglas Yong, Dr. Todd Martin and Dr. Wiliam Barret from US-EPA for several helpful explanations on WAR algorithm. Financial support from CNPq-Brazil and PETROBRAS S.A. is acknowledged by O. Q. F. Araujo and J. L. Medeiros.

NOMENCLATURE

<i>CDF</i>	cumulative distribution function
<i>iCDF</i>	inverse of cumulative distribution function
<i>PDF</i>	probability density function
$\bullet^{(cp)}$ <i>I_{in}</i>	input rate of potential environment impact of chemical process
$\bullet^{(cp)}$ <i>I_{out}</i>	output rate of potential environment impact of chemical process
$\bullet^{(ep)}$ <i>I_{in}</i>	input rate of potential environment impact of energy generation process
$\bullet^{(ep)}$ <i>I_{out}</i>	output rate of potential environment impact of energy generation process
$\bullet^{(cp)}$ <i>I_{we}</i>	potential environment impact output rate with waste energy from chemical process
$\bullet^{(ep)}$ <i>I_{we}</i>	potential environment impact output rate with waste energy from energy generation process
$\bullet^{(t)}$ <i>I_{gen}</i>	potential environment impact generation rate in chemical process and power plant
\bullet <i>M_{j,l}</i>	mass flow rate of stream <i>j</i>
<i>x_{kj}</i>	mass fraction of component <i>k</i> in stream <i>j</i>
(Score) _{<i>ki</i>}	impact score of species <i>k</i> in environmental impact category <i>i</i>
<(Score) _{<i>k</i>} > _{<i>i</i>}	average score of all species in environmental impact category <i>i</i>
$\underline{\underline{P}}_{n \times n}$	matrix of orthonormal eigenvectors of $\underline{\underline{R}}_X$
$\underline{\underline{P}}_{i \times 1}$	eigenvector <i>i</i> of $\underline{\underline{R}}_X$
$\underline{\underline{R}}_{n \times n}$	sample variance-covariance matrix of $\underline{\underline{X}}$
$\underline{\underline{S}}_{i \times 1}$	vector of generalized scores <i>S</i> ₁ , <i>S</i> ₂ , ..., <i>S</i> _{<i>n</i>} from <i>X</i> ₁ , <i>X</i> ₂ , ..., <i>X</i> _{<i>n</i>}
$\underline{\underline{X}}_{m \times n}$	matrix of process data with <i>n</i> scalar variables and <i>m</i> samples

Greek letters

α_i	weighting factor for environmental impact category i
λ_i	eigenvalue i of $\underline{\underline{R}}_x$
$\underline{\lambda}_{n \times 1}$	column vector of positive eigenvalues of $\underline{\underline{R}}_x$
μ	mean both as a population parameter and as a sample statistics
σ	standard deviation both as a population parameter and as a sample statistics
ψ_{ki}^s	specific potential environment impact of species k in environmental impact category i

Abbreviations

CAE	Computer Aided Engineering
EOR	Enhanced Oil Recovery
EOS	Equation of State
GOR	Gas-to-Oil Ratio
HCDP	Hydrocarbons Dew-Point
HCDPA	Hydrocarbons Dew-Point Adjustment
JTE	Joule-Thomson Expansion
MC	Monte Carlo
MCMC	Markov Chain Monte Carlo
MM Nm ³ /d	Millions of normal cubic meters per day
MM Sm ³ /d	Millions of standard cubic meters per day
MP	Membrane Permeation
NG	Natural Gas
TEG	Triethylene Glycol
WAR	Waste Reduction Algorithm
WDP	Water Dew-Point
WDPA	Water Dew-Point Adjustment

REFERENCES

1. BP Statistical Review of World Energy 2017, Br. Pet., No. 66, pp 1-52, 2017, <http://www.bp.com/content/dam/bp/en/corporate/pdf/energy-economics/statistical-review-2017/bp-statistical-review-of-world-energy-2017-full-report.pdf>, [Accessed: 13-August-2018]
2. Araújo, O. de Q. F., Reis, A. de C., de Medeiros, J. L., do Nascimento, J. F., Grava, W. M. and Musse, A. P. S., Comparative Analysis of Separation Technologies for Processing Carbon Dioxide Rich Natural Gas in Ultra-deepwater Oil Fields, *J. Clean. Prod.*, Vol. 155, Part 1, pp 12-22, 2017, <https://doi.org/10.1016/j.jclepro.2016.06.073>
3. Fleshman, J., Alderton, P., Bahnassi, E. and Khouri, A. R., Achieving Product Specifications for Ethane through to Pentane Plus from NGL Fractionation Plants, *Proceedings of the AIChE Annu. Meet.*, Cincinnati, Ohio, USA, 2005.
4. Arellano-Garcia, H. and Wozny, G., Chance Constrained Optimization of Process Systems Under Uncertainty: I. Strict Monotonicity, *Comput. Chem. Eng.*, Vol. 33, No. 10, pp 1568-1583, 2009, <https://doi.org/10.1016/j.compchemeng.2009.01.022>
5. Diaz, S., Brignole, E. A. and Bandoni, A., Flexibility Study on a Dual Mode Natural Gas Plant in Operation, *Chem. Eng. Commun.*, Vol. 189, No. 5, pp 37-41, 2002, <https://doi.org/10.1080/00986440211744>
6. Mesfin, G. and Shuhaimi, M., A Chance Constrained Approach for a Gas Processing Plant with Uncertain Feed Conditions, *Comput. Chem. Eng.*, Vol. 34, No. 8, pp 1256-1267, 2010, <https://doi.org/10.1016/j.compchemeng.2010.03.009>

7. Getu, M., Mahadzir, S., Samyudia, Y., Khan, M. S., Bahadori, A. and Lee, M., Risk-based Optimization for Representative Natural Gas Liquid (NGL) Recovery Processes by Considering Uncertainty from the Plant Inlet, *J. Nat. Gas Sci. Eng.*, Vol. 27, Part 1, pp 42-54, 2015, <https://doi.org/10.1016/j.jngse.2015.01.028>
8. Li, P., Wendt, M. and Wozny, G., Optimal Production Planning for Chemical Processes under Uncertain Market Conditions, *Chem. Eng. Technol.*, Vol. 27, No. 6, pp 641-651, 2004, <https://doi.org/10.1002/ceat.200400048>
9. Gozalpour, F., Ren, S. R. and Tohidi, B., CO₂ EOR and Storage in Oil Reservoir, *Oil Gas Sci. Technol.*, Vol. 60, No. 3, pp 537-546, 2005, <https://doi.org/10.2516/ogst.2005036>
10. Gonzaga, C. S. B., A Monte Carlo Methodology for Offshore Natural Gas Processing Project (in Portuguese), *M.Sc. Thesis*, School of Chemistry, Federal University of Rio de Janeiro, Rio de Janeiro, Brasil, 2014.
11. Dzobo, O., Gaunt, C. T. and Herman, R., Investigating the use of Probability Distribution Functions in Reliability-worth Analysis of Electric Power Systems, *Int. J. Electr. Power Energy Syst.*, Vol. 37, No. 1, pp 110-116, 2012, <https://doi.org/10.1016/j.ijepes.2011.12.013>
12. Tula, A. K., Babi, D. K., Bottlaender, J., Eden, M. R. and Gani, R., A Computer-aided Software-tool for Sustainable Process Synthesis-intensification, *Comput. Chem. Eng.*, Vol. 105, pp 74-95, 2017, <https://doi.org/10.1016/j.compchemeng.2017.01.001>
13. Bakshi, B. R. and Fiksel, J., The Quest for Sustainability?: Challenges for Process Systems Engineering, *AIChE Journal*, Vol. 49, No. 6, pp 1350-1358, 2003, <https://doi.org/10.1002/aic.690490602>
14. Wan Ahmad, W. N. K., Rezaei, J., de Brito, M. P. and Tavasszy, L. A., The Influence of External Factors on Supply Chain Sustainability Goals of the Oil and Gas Industry, *Resour. Policy*, Vol. 49, pp 302-314, 2016, <https://doi.org/10.1016/j.resourpol.2016.06.006>
15. Sikdar, S. K., Sustainability Metrics, *AIChE Journal*, Vol. 49, No. 8, pp 1928-1932, 2003, <https://doi.org/10.1002/aic.690490802>
16. Araújo, O. de Q. F., de Medeiros J. L., Yokoyama, L. and Morgado, C. R. V., Metrics for Sustainability Analysis of Post-combustion Abatement of CO₂ Emissions: Microalgae Mediated Routes and CCS (Carbon Capture and Storage), *Energy*, Vol. 92, Part 3, pp 556-568, 2015, <https://doi.org/10.1016/j.energy.2015.03.116>
17. Sikdar, S. K., Sengupta, D. and Mukherjee, R., *Measuring Progress Towards Sustainability*, Springer, Cham, Switzerland, 2016.
18. Cabezas, H., Bare, J. C. and Mallick, S. K., Pollution Prevention with Chemical Process Simulators: The Generalized Waste Reduction (WAR) Algorithm – Full Version, *Comput. Chem. Eng.*, Vol. 23, No. 4-5, pp 623-634, 1999, [https://doi.org/10.1016/S0098-1354\(98\)00298-1](https://doi.org/10.1016/S0098-1354(98)00298-1)
19. Young, D. M. and Cabezas, H., Designing Sustainable Processes with Simulation: The Waste Reduction (WAR) Algorithm, *Comput. Chem. Eng.*, Vol. 23, No. 10, pp 1477-1491, 1999, [https://doi.org/10.1016/S0098-1354\(99\)00306-3](https://doi.org/10.1016/S0098-1354(99)00306-3)
20. Young, D., Scharp, R. and Cabezas, H., The Waste Reduction (WAR) Algorithm: Environmental Impacts, Energy Consumption, and Engineering Economics, *Waste Manag.*, Vol. 20, No. 8, pp 605-615, 2000, [https://doi.org/10.1016/S0956-053X\(00\)00047-7](https://doi.org/10.1016/S0956-053X(00)00047-7)
21. Roffel, B. and Betlem, B., *Process Dynamics and Control: Modeling for Control and Prediction*, John Wiley & Sons Inc., New Jersey, USA, 2006.
22. Bahadori, A. and Vuthaluru, H. B., Rapid Estimation of Equilibrium Water Dew Point of Natural Gas in TEG Dehydration Systems, *J. Nat. Gas Sci. Eng.*, Vol. 1, No. 3, pp 68-71, 2009, <https://doi.org/10.1016/j.jngse.2009.08.001>
23. Netusil, M. and Ditzl, P., Comparison of Three Methods for Natural Gas Dehydration, *J. Nat. Gas Chem.*, Vol. 20, No. 5, pp 471-476, 2011,

- [https://doi.org/10.1016/S1003-9953\(10\)60218-6](https://doi.org/10.1016/S1003-9953(10)60218-6)
24. Reis, A. de C., de Medeiros, J. L., Nunes, G. C. and Araújo, O. de Q. F., Upgrading of Natural Gas Ultra-rich in Carbon Dioxide: Optimal Arrangement of Membrane Skids and Polishing with Chemical Absorption, *J. Clean. Prod.*, Vol. 165, pp 1013-1024, 2017, <https://doi.org/10.1016/j.jclepro.2017.07.198>
 25. Kamal, M. S., Hussein, I. A., Sultan, A. S. and Von Solms, N., Application of Various Water Soluble Polymers in Gas Hydrate Inhibition, *Renew. Sustain. Energy Rev.*, Vol. 60, pp 206-225, 2016, <https://doi.org/10.1016/j.rser.2016.01.092>
 26. Arinelli, L. O., Trotta, T. A. F., Teixeira, A. M., de Medeiros, J. L. and Araújo, O. de Q. F., Offshore Processing of CO₂ Rich Natural Gas with Supersonic Separator versus Conventional Routes, *J. of Nat. Gas Sci. and Eng.*, Vol. 46, pp 199-221, 2017, <https://doi.org/10.1016/j.jngse.2017.07.010>
 27. Hastings, W. K., Monte Carlo Sampling Methods using Markov Chains and their Applications, *Biometrika*, Vol. 57, No. 1, pp 97-109, 1970, <https://doi.org/10.2307/2334940>
 28. Jacques, S., Monte Carlo Sampling of Probability Distributions: How to Make the Computer Roll Dice, Oregon Medical Laser Center, 1998, <https://omlc.org/news/sep98/montecarlosampling/index.html>, [Accessed: 04-February-2018]
 29. Abramowitz, M. and Stegun, I. A., Handbook of Mathematical Functions with Formulas, Graphs and Mathematical Tables (National Bureau of Standards Applied Mathematics Series No. 55), *Dover Publications*, Vol. 32, No. 1, pp 239, 1965.
 30. Caflisch, R. E., Monte Carlo and Quasi-Monte Carlo Methods, *Acta Numerica*, Vol. 7, pp 1-49, 1998, <https://doi.org/10.1017/S0962492900002804>
 31. Lemieux, C., *Monte Carlo and Quasi-Monte Carlo Sampling*, Springer, Berlin, Germany, 2009.
 32. Sepiacci, P., Depetri, V. and Manca, D., A Systematic Approach to the Optimal Design of Chemical Plants with Waste Reduction and Market Uncertainty, *Comput. Chem. Eng.*, Vol. 102, pp 96-109, 2017, <https://doi.org/10.1016/j.compchemeng.2016.11.032>
 33. Clift, R., Sustainable Development and its Implications for Chemical Engineering, *Chem. Eng. Sci.*, Vol. 61, No. 13, pp 4179-4187, 2006, <https://doi.org/10.1016/j.ces.2005.10.017>
 34. Jiménez-González, C., Kim, S. and Overcash, M. R., Methodology for Developing Gate-to-gate Life Cycle Inventory Information, *Int. J. Life Cycle Assess.*, Vol. 5, No. 3, pp 153-159, 2000, <https://doi.org/10.1007/BF02978615>
 35. Barrett, W. M., van Baten, J. and Martin, T., Implementation of the Waste Reduction (WAR) Algorithm Utilizing Flowsheet Monitoring, *Comput. Chem. Eng.*, Vol. 35, No. 12, pp 2680-2686, 2011, <https://doi.org/10.1016/j.compchemeng.2011.02.004>

Paper submitted: 26.03.2018
Paper revised: 13.08.2018
Paper accepted: 16.08.2018